Available online at www.sciencedirect.com

SciVerse ScienceDirect

Ceramics International 39 (2013) 3211–3219

CERAMICS INTERNATIONAL

www.elsevier.com/locate/ceramint

Palladium–alumina composite membrane for hydrogen separator fabricated by combined sol–gel, and electroless plating technique

Ratna Sari[a,b,c,*], Zahira Yaakob[a,b], Manal Ismail[a,b], Wan Ramli Wan Daud[a,b], Lukman Hakim[a,b,d]

[a]*Fuel Cell Institute, Universiti Kebangsaan Malaysia, 43600 Bangi, Selangor, Malaysia*

[b]*Department of Chemical and Process Engineering, Faculty of Engineering and Built Environment, Universiti Kebangsaan Malaysia, 43600 UKM Bangi, Selangor, Malaysia*

[c]*Lhokseumawe State Polytechnic, 24301 Lhokseumawe, North Aceh, Indonesia*

[d]*Malikussaleh University, 141 Reuleut, North Aceh, Indonesia*

Received 17 July 2012; received in revised form 24 September 2012; accepted 1 October 2012
Available online 17 October 2012

Abstract

In this work, the performance of a novel coating of palladium over an alumina ceramic membrane was studied to enhance the hydrogen selectivity produced by an ethanol steam reforming reaction. Preparation of the palladium coated ceramic alumina membrane tube was performed using a combined sol–gel process and an electroless plating technique. Characterisation of the membrane was conducted using SEM and AFM. The palladium–alumina membrane was housed in the module membrane, and then packed with CuO–ZnO commercial catalyst to carry out the ethanol steam reforming reaction in a solid–gas phase. The reaction temperature and H_2O/C_2H_5OH feed molar ratio of the feed reactants were maintained at 573 K and 13:1, respectively. The reactions were then conducted at various reaction pressures in the range of 1.08–1.38 bar and WHSV of either 37 or 74 h^{-1}. Their effects upon ethanol conversion, hydrogen recovery, hydrogen yield and hydrogen selectivity were investigated. At 1.38 bar with WHSV 37 h^{-1}, the maximum of ethanol conversion (61.5%), hydrogen recovery (42.82%), hydrogen yield (26.75%) and hydrogen selectivity (92.6%) have been measured.

Keywords: Palladium–alumina composite; Hydrogen; Electroless plating

1. Introduction

As a green fuel, hydrogen has been playing an important role for the latest decade. Ready availability of efficient fuel would mitigate CO_2 emissions and alleviate the problems associated with global warming [1,2]. Ethanol is one renewable energy source for hydrogen production. It has several advantages in that it can be obtained easily and, as an agroproduct, is cheap, non-toxic, biodegradable and easy to handle [3]. Hydrogen is inherently produced from ethanol in steam reforming processes [4].

Ongoing advances in fuel cell technologies, as well as the demand for purified hydrogen, have led to the development of the membrane reactor (MR). The MR is a hybrid form that combines reactor and separator in a single unit that enhances ethanol conversion by the removal of hydrogen, resulting in a shift toward the productive reaction while achieving an equilibrium state. Combining MR with membrane technology enables operating at lower energy consumption, and reduces the operational and maintenance cost; hence it is an economically viable technology [5].

Recent efforts to increase hydrogen permeation rates have led to the development of palladium (Pd)-based composite membranes [6]. These composite membranes consist of a dense thin layer of Pd or a Pd alloy on a porous support. Porous glass, ceramic or stainless steel in the form of tubes or discs can be employed as supports [7,8]. The interdiffusion problem, surface roughness and pore size of stainless steel

*Corresponding author at: Fuel Cell Institute, Universiti Kebangsaan Malaysia, 43600 Bangi, Selangor, Malaysia. Tel.: +60 389216050; fax: +60 389216024.

E-mail addresses: ratna@eng.ukm.my (R. Sari), zahira@eng.ukm.my (Z. Yaakob), manal@eng.ukm.my (M. Ismail), wramli@gmail.com (W.R.W. Daud), hakim@eng.ukm.my (L. Hakim).

0272-8842/$ - see front matter © 2012 Elsevier Ltd and Techna Group S.r.l. All rights reserved.
http://dx.doi.org/10.1016/j.ceramint.2012.10.006

may limit its applications. Porous ceramic has been an efficient support, providing a structure possessing both high hydrogen fluxes and good mechanical properties; it is also inexpensive [9]. Pd ceramic composite membranes can be formed by deposition such as chemical vapor deposition, electroplating, sol–gel or electroless plating [10–12].

To form a thin continuous membrane without defects, the support surface should be smooth. A problem with an α-alumina membrane support was surface roughness. To reduce surface roughness, an intermediate layer was necessary. Therefore it is necessary to use a sol–gel derived γ-alumina support. A Pd film with good adhesion could be coated on a sol–gel γ-alumina support, but not on an α-alumina support [13].

In recent years, use of sol–gel processes to obtain thin films has grown rapidly due to the simplicity of this procedure [14]. In the sol–gel technique, a sol is prepared using an organo-metallic oxide, which undergoes hydrolysis and condensation polymerization reactions to give gels. Hydrogen permeation studies through asymmetric Pd–alumina composite membranes obtained from sol–gel techniques have been reported in the literature [15,16]. Few authors have reported the permeability of gases across alumina–titania tube membranes [17,18].

The preparation of membranes by means of electroless plating techniques is widely used for uniform deposition of the active layer on substrates with a variety of complex geometries and large surface areas. The hardness of the deposited layer and its strong adhesion to the support, as well as the simplicity of the procedure, which make it easy to scale-up, can be considered some of the advantages of electroless plating [19].

Several studies have described ethanol steam reforming (ESR) processes in Pd-based composite membrane reactors. Lim et al. [20] carried out ESR in a silica-alumina membrane, and found that ethanol conversion and hydrogen selectivity were 86% and 71.1% at 623 K, with variations in contact time. Basile et al. [21] studied ESR in Pd-porous stainless steel (PSS) and obtained an ethanol conversion ranging from 85.0 to 100%, and a hydrogen selectivity of 65%, at a temperature of 673 K and pressure of 3.0 to 8.0 bars. Iulianelli et al. [22] performed ESR in Pd–Ag/PSS. The ethanol conversion and hydrogen selectivity were 95% and 64% at a temperature of 673 K and a reaction pressure of 1.5 bar. However, no publication has reported the use of Pd-alumina membrane tube in MR for hydrogen production and purification by ESR. The present work applied a Pd–alumina membrane reactor to steam reforming of ethanol. Hydrogen permeation from the reaction side through the Pd–alumina membrane was expected to enhance the ethanol conversion at a competitive hydrogen selectivity.

2. Experimental procedure

2.1. Materials

Alpha-Alumina membrane tubing with an outer diameter, length, thickness and pore size of 1 cm, 17.5 cm, 0.2 cm and 100 nm, respectively, was supplied by Jiangsu Jiuwu Hitech Co. Ltd. The chemicals used in the sol solutions were analytical grade materials, i.e. aluminium nitrate nonahydrate (98%, Fluka), nitrate acid (65% Merck), poly vinyl alcohol (98%, Merck). The sensitization solution was tin (II) chloride (Sigma-Aldrich) and hydrochloric acid (37%, Merck). The activation solution was palladium chloride (99.9%, Aldrich) and hydrochloric acid (37%, Merck). The electroless plating solution consisted of palladium chloride (99.9%, Aldrich), sodium hypophosphite anhydrous (Sigma-Aldrich), ethylene diamine tetraacetic acid (Sigma), and ammonium hydroxide (28%, Sigma-Aldrich).

2.2. Membrane preparation

2.2.1. Gamma–alumina coating by a sol–gel process

The alpha-alumina membrane tube was cleaned by sequential ultrasonic rinsing in 0.1% sodium hydroxide for 1 min, followed by 100 mL deionized water for 2 min, rinsing in 100 mL isopropanol for 10 min, and finally in 100 mL deionized water for 10 min. It was then dried in an oven at 393 K for at least 8 h. The second step was preparation of the Pd–alumina membrane by a sol–gel technique [23]. To do this, appropriate amounts of deionized water were heated to 353–363 K, with subsequent addition of aluminium nitrate nonahydrate, nitric acid, and poly vinyl alcohol; temperature was maintained at 353–363 K. The solution (Table 1) was thoroughly mixed at 353–363 K for 24 h under reflux conditions before immersing the membrane for 3 h for plating; then it was dried at 393 K for 2 h.

2.2.2. Pd coating with an electroless plating technique

The sensitization and activation of the membrane were carried out at room temperature at pH 4–5. Prior to this process, the membrane tube was sealed at one end with glass enamel (Aremco 617) and at the other end with Teflon stick to ensure activation took place on the outer membrane surface only. The membrane was immersed into a sensitization solution of $SnCl_2$ (1 g/L) and HCl (1 mL/L) for 2 min, and then washed with deionized water for 30 s; it was then immersed into the activation solution of $PdCl_2$ (0.09 g/L) and HCl (1 mL/L) for another 2 min. After that, it was washed with deionized water again for 30 s. This cycle was repeated ten times. The electroless plating solution consisted of $PdCl_2$, NH_4OH, EDTA, and $NaPO_2H_2$ (Table 2). The plating process was carried out at room temperature, pH 11 and a speed of membrane rotation of 78 rpm on a Heidolp RZR 2021 for 7 h, then

Table 1
Sol–gel solution.

Component	Composition
Aluminium nitrate nonahydrate	18.76 g
Nitrate acid	3.1 mL
Poly vinyl alcohol	2.1 mL
Deionized water	90.3 mL

repeated six times. The ceramic membrane with a layer of Pd coating was then heated at 373 K overnight and stored in the desiccator to protect it from ambient humidity.

2.3. Characterisation

The cross-sectional image, thickness and morphology of the Pd composite membrane were analysed using a scanning electron microscopy (SEM, LEO 1450VP Zeiss) while the atomic force microscopy (AFM) image of the membrane morphology was analysed by AFM Ntegra Prima NT-MDT.

2.4. Hydrogen permeation test unit

The gas permeation tests were carried out at a temperature of 573 K and a range of pressures (1.08–1.38 bar). The gas flow rate was 137 mL min^{-1}. The effective area of the membrane for permeation was 9.42 cm^2. The permeated gas flow rates were measured using a digital flow meter (Agilent technologies ADM2000) at constant temperature with pressure difference across the membrane. Membranes were characterised by conducting permeation experiments with hydrogen and nitrogen.

2.5. Ethanol steam reforming (ESR) reaction and hydrogen selectivity test unit

The MR comprised a palladium–alumina membrane module 16 cm in length, with a diameter of 1.18 cm. In the MR, Pd–alumina membrane was reduced with hydrogen in a furnace at 673 K for 4 h. The CuO–ZnO commercial catalyst was packed in the membrane zone. Reaction temperature was 573 K and the reaction pressures were 1.08–1.38 bar. The weight hourly space velocities (WHSV) were 37 h^{-1} and 74 h^{-1}, while the ethanol/H_2O feed ratio was kept at 1:13. The liquid reactants were mixed and vaporized, and then fed into the MR. For the ESR test, the concentrations of permeate and retentate gases were analysed by a gas chromatograph (GC) (Clarus 500 Perkin Elmer), and the flow rate of the retentate and permeate gases were measured using a soap bubble flow meter and digital flow meter (Agilent technologies ADM2000). The ethanol concentration in the retentate gas was analysed by high performance liquid chromatography (HPLC) (Egilent Technologies 1200 Series). Ethanol conversion, hydrogen recovery, hydrogen yield and hydrogen selectivity were the parameters used for describing the Pd–alumina MR's performance. An image and schematic diagram of the Pd–alumina MR Systems are shown in Fig. 1.

Table 2
Electroless plating solution.

Component	Composition
$PdCl_2$	0.27 wt%
NH_4OH (28%)	58.5 mL
$NaPO_2H_2$	0.02 wt%
EDTA	5.25 g

The main reaction of the ethanol steam reforming process is represented by the following:

$$C_2H_5OH + 3H_2O \leftrightarrow 6H_2 + 2CO_2 \text{(Ethanol steam reforming reaction)} \quad (1)$$

The reactions mechanisms are the simultaneous decomposition and water–gas shift reaction, as follows:

$$C_2H_5OH \leftrightarrow CO + CH_4 + H_2 \text{(Ethanol dehydrogenation reaction)} \quad (2)$$

$$CO + H_2O \leftrightarrow CO_2 + H_2 \text{(Water gas shift reaction)} \quad (3)$$

Ethanol conversion, hydrogen selectivity, hydrogen recovery and hydrogen yield were used to evaluate the

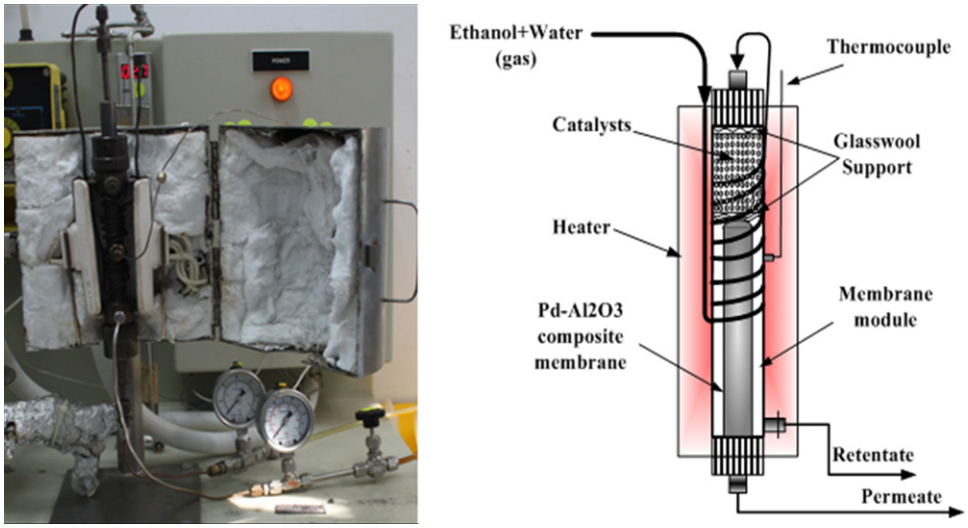

Fig. 1. Image and schematic of the Pd–alumina MR system.

performance of the Pd–alumina MR, defined as:

$$C_2H_5OH\ conversion, \times (\%) = \frac{(C_2H_5OH)_{in} - (C_2H_5OH)_{out}}{(C_2H_5OH)_{in}} \times 100 \quad (4)$$

$$P\ selectivity,\ S\ (\%) = \frac{P_{out}}{(H_2 + CO + CO_2 + CH_4)_{out}} \times 100 \quad (5)$$

where P is H_2, CO, CO_2 or CH_4.

$$Hydrogen\ Recovery, R\ (\%) = \frac{H_{2,permeate}}{H_{2,permeate} + H_{2,retentate}} \times 100 \quad (6)$$

$$Hydrogen\ Yield, Y\ (\%) = \frac{H_{2,permeate}}{6C_2H_5OH_{in}} \times 100 \quad (7)$$

3. Results and discussion

3.1. Thickness and morphology membrane

Fig. 2 (a) illustrates the cross-sectional three-layer Pd–alumina composite ceramic membrane. This is evidenced by the sharp, clean interface between layers. The small gamma-alumina membrane precursor particles penetrated into the pores of the alpha-alumina support, and the separating layer of Pd film is adhered to the gamma–alumina layer. The thicknesses of the Pd and gamma–alumina layers were 7.146 and 20.1 μm, respectively. Fig. 2 (b) reveals the surface morphology of the prepared membrane. Fine Pd was deposited on top of the macroporous alumina membrane support, and formed a smooth layer.

Fig. 3 shows an AFM surface micrograph for the Pd membrane. The Pd membrane has an average pore of size 0.00784 μm. The average roughness of the Pd membrane was 0.030626 μm, consisting of small grains with a mean grain diameter of 0.009702 μm. The small grain size minimised the roughness of the Pd membrane.

3.2. Hydrogen permeation

The rate of hydrogen permeation 'J' can be expressed as;

$$J_{H_2} = \frac{Q}{d}\left(P^n_{1\ retentate} - P^n_{2\ permeate}\right) \quad (8)$$

where Q is the hydrogen permeability (mol m^{-1} s^{-1} bar^{-n}), d is the thickness of the membrane (m), P_1 and P_2 are the hydrogen partial pressure in the retentate and permeate (bar), and n is the pressure dependence factor (0.5–1). The factor n is equal to 0.5 when the pressure is relatively low, and the diffusion is assumed to be the rate-limiting step. At high pressure, n becomes equal to 1, and the hydrogen–hydrogen interactions in the palladium bulk are not negligible [24]. Fig. 4 shows the influence of reaction pressure on the hydrogen permeation flux at a temperature of 573 K by varying n. It can be observed from the Fig. 4 that the highest linear regression value (R^2) is obtained at $n=0.5$. Therefore, it follows Sieverts' law and Eq. (8) becomes:

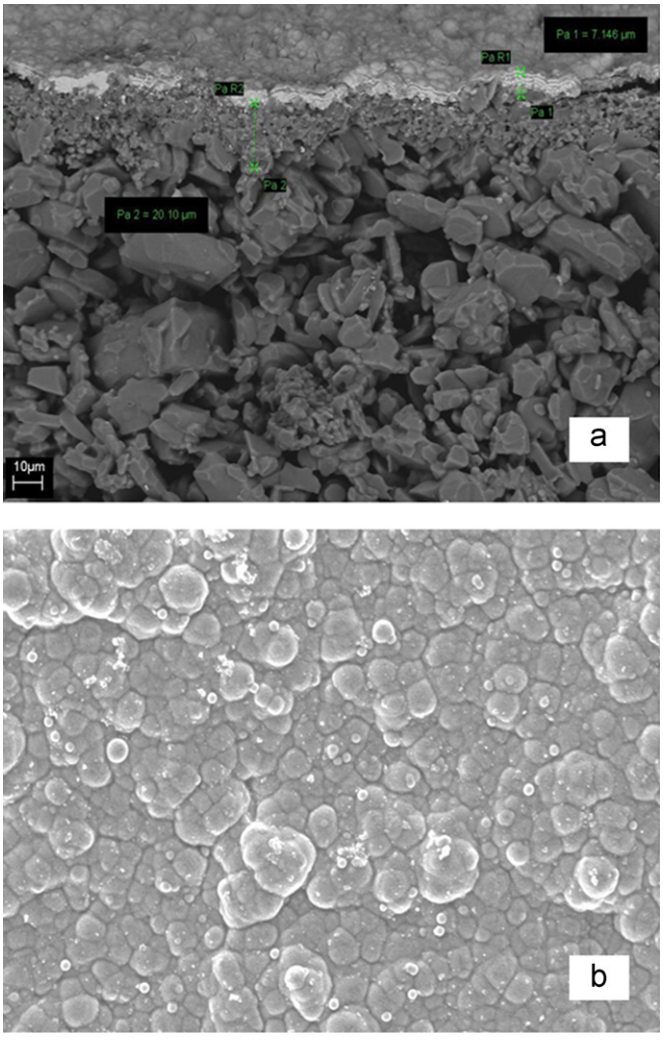

Fig. 2. (a) Thickness of Palladium and gamma alumina membrane, and (b) palladium membrane morphology.

$$J_{H_2} = \frac{Q}{d}\left(P^{0.5}_{1\ retentate} - P^{0.5}_{2\ permeate}\right) \quad (9)$$

Under the investigated condition, the n value 0.5 indicated that bulk diffusion is slower than surface rate (adsorption/desorption). The increase of reaction pressure will lead to the improvement of surface rate on the feed side and then the surface resistance will become less significant compared to the bulk diffusion in the metal layer. Therefore according to Sieverts' law, hydrogen permeation increased with increasing reaction pressure. This observation is supported by similar findings from Collins et al. [25] for Pd–alumina with pore size of the support 10–200 nm and thickness 11.4 μm, the n-value was 0.58.

N_2 permeation tests were performed in order to check the presence of any defect in the Pd layer. The ideal H_2/N_2

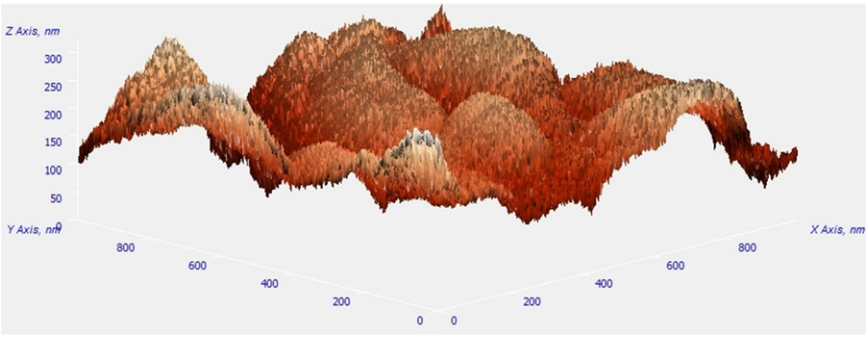

Fig. 3. Atomic force microscopy (AFM) image of Palladium–alumina composite membrane.

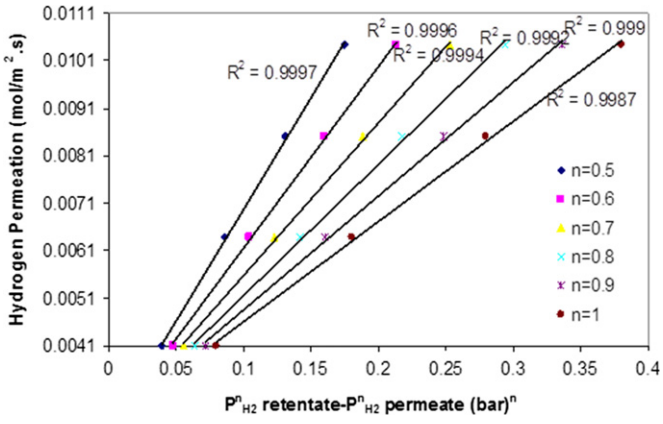

Fig. 4. Hydrogen permeation versus reaction pressure at 573 K for different n factors.

selectivity, defined as the ratio of the hydrogen flux to nitrogen can be expressed as follows:

$$\alpha_{H_2/N_2} = \frac{F_{H_2}}{F_{N_2}} \tag{10}$$

Four data were taken and the H_2/N_2 selectivity was plotted as a function of the difference between pressure in the retentate and permeate sides at temperature 573 K (Fig. 5). Data obtained for Pd–alumina membrane indicated that the ideal H_2/N_2 selectivity (α_{H_2/N_2}) decreases with increasing pressure difference. This can be explained by following equations that assume the existence of defects through which Knudsen diffusion happens. The total hydrogen flux is sum of fluxes through the Pd membrane and defects:

$$F^T_{H_2} = J_{H_2} + F^K_{H_2} \tag{11}$$

where $J_{H_2}$is the hydrogen flux through a defect-free Pd–alumina membrane given by Eq. (9) and $F^K_{H_2}$ is the Knudsen diffusion flux of hydrogen. Both hydrogen and nitrogen diffuse through defects given by:

$$F^K_i = \frac{D^K_i}{RTL}\Delta P \tag{12}$$

where D^K_i is Knudsen diffusivity, T the temperature, and L is thickness of the membrane. Eq. (10) can be written as:

$$\alpha_{H_2/N_2} = \frac{F^T_{H_2}}{F^K_{N_2}} = \frac{F^K_{H_2} + J_{H_2}}{F^K_{N_2}} \tag{13}$$

The ratio of the hydrogen and nitrogen Knudsen fluxes is given by:

$$\frac{F^K_{H_2}}{F^K_{N_2}} = \frac{\sqrt{M_{N_2}}}{\sqrt{M_{H_2}}} = 3.74 \tag{14}$$

where M is the molecular weight of gas. The expression for α_{H_2/N_2} can then be re-expressed as:

$$\alpha_{H_2/N_2} = 3.74 + \frac{Q\,R\,T\,L\,\Delta P^{0.5}}{d\,D^K_{N_2}\Delta P} \tag{15}$$

It is noted from Eq. (15) that the nitrogen flux is proportional to ΔP whereas the hydrogen flux is proportional to $\Delta P^{0.5}$. The nitrogen flux increases at a faster rate than that hydrogen flux, and as a result, the ideal H_2/N_2 selectivity (α_{H_2/N_2}) decreases with increasing pressure difference. According to Guazzone et al. [26], leak development in fresh Pd composite membranes that the Pd layer deposited by the electroless deposition method will always, and in an inherently manner, occur at temperatures higher than 673–723 K. Results of H_2/N_2 selectivity done by Dittmeyer et al. at 673 K with thickness 7–15 μm were 100–1000 [27]. The H_2/N_2 selectivity obtained in this study was above 184, therefore, results in a good agreement with Dittmeyer et al. [27]. It does mean that the composite membrane used in this experiment has comparable performance to that of other Pd–alumina membrane [27].

3.3. Effect of WHSV and reaction pressure

Weight hourly space velocity (WHSV) is a convenient capacity measure for chemical reactors, and is frequently used to relate to reactor performance. Its reciprocal is the contact time. Permeate selectivities are shown at two different WHSV in Table 3.

Hydrogen selectivity was found to decrease with increasing WHSV. The WHSV is increased from 37 h^{-1} to 74 h^{-1} at a reaction pressure of 1.38 bar, the hydrogen selectivity is decreased from 92.6% to 91.3%. It decreased the CO_2

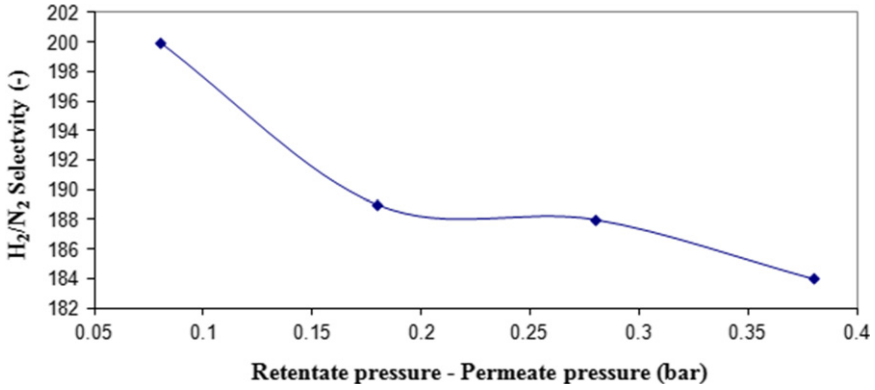

Fig. 5. H_2/N_2 selectivity for different pressure at 573 K.

Table 3
Selectivities of permeate products at a reaction temperature of 573 K and pressure. of 1.38 bar.

WHSV (h^{-1})	S_{H2} (%)	S_{CO2} (%)	S_{CH4} (%)	S_{CO} (%)
37	92.6	3.33	0	4.07
74	91.3	2.04	0	6.66

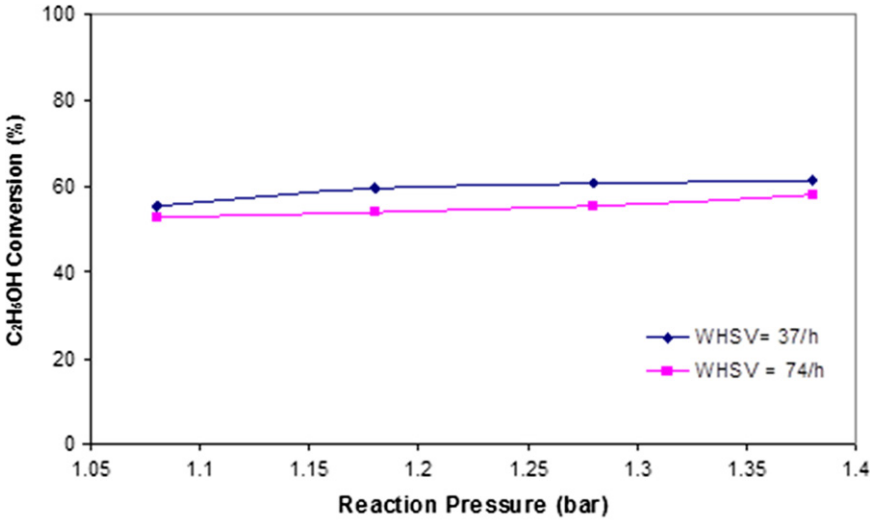

Fig. 6. Ethanol conversion versus reaction pressure at different WHSV.

selectivity from 3.33% to 2.04%, and increased the CO selectivity from 4.07% to 6.66%. The decrease in hydrogen and CO_2 selectivity and increase in CO selectivity with increasing WHSV was explained by shorter resident time and consequently decrease contact time. These phenomena also affected the ethanol conversion. The ethanol conversion was obtained from the ratio of ethanol consumed and ethanol fed into the membrane reactor. Increasing the WHSV from 37 to 74 h^{-1} at a reaction pressure of 1.38 bar decreased the ethanol conversion from 61.5% to 55.3% (Fig. 6). The ethanol conversion increased with increasing reaction pressure, due to the higher pressure encourages on ethanol conversion. Larger increases in hydrogen recovery and hydrogen yield were also observed with increasing reaction pressure, because the continuous removal of hydrogen during the reaction shifted the equilibrium to the products. These phenomena occurred because of Le Chatelier principle. Hydrogen and CO_2 concentration increase with the pressure which Basile et al. reported [21]

Fig. 7 shows ethanol conversion in the MR and the packed-bed reactor (PBR) at 573 K for different reaction pressure. The PBR operation condition same with the MR except no permeable Pd–alumina membrane tube herein. Ethanol conversions were obtained in the MR higher than the PBR for all reaction pressures because hydrogen pass away through the Pd–alumina membrane during the

reaction make equilibrium shift to favour the product. Improved ethanol conversion in the MR was 20–35% for reaction pressure 1.08–1.38 bar.

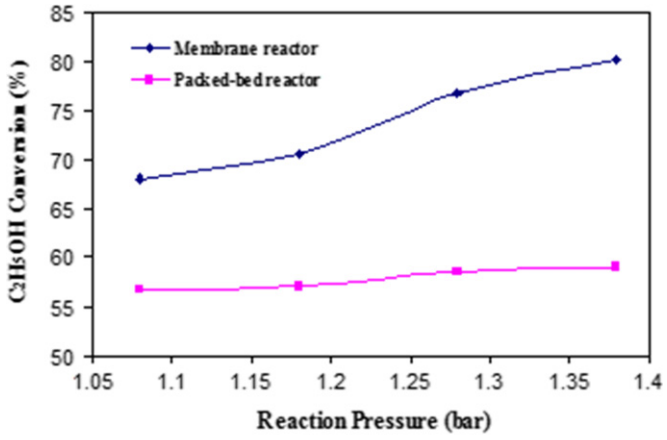

Fig. 7. Ethanol conversion in the MR and the PBR at different reaction pressure.

Indications of the effects of WHSV on the performance of the Pd–alumina MR also can be seen in Figs. 8 and 9.

These figs. show the same trend win which, as the WHSV is increased from 37 h^{-1} to 74 h^{-1} at a reaction pressure of 1.08 bar, the hydrogen recovery and hydrogen yield are decreased from 11.56% to 4.48%, and from 8.89% to 2.11%, respectively. At a low WHSV, the hydrogen recovery and hydrogen yield are high, because contact time between catalyst and ethanol is long and make the rate of the ESR reaction is high. The continuous removal of hydrogen from the reaction site by the Pd–alumina membrane does affect the reaction conversion (and therefore the hydrogen recovery and hydrogen yield) to any significant degree.

3.4. The activation energy

The correlation between temperature and hydrogen permeability can be expressed by an Arrhenius-like equation as follows:

$$Q = Q_0 \exp(-E_a/RT) \quad (16)$$

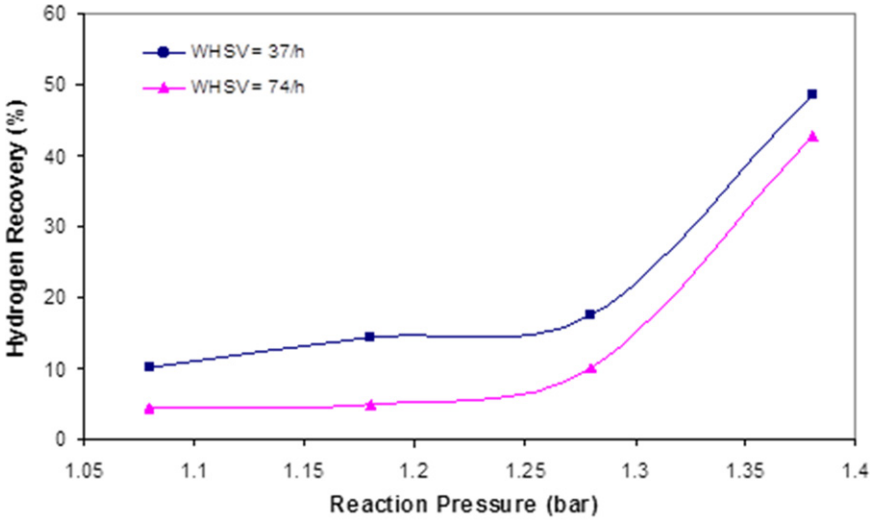

Fig. 8. Hydrogen recovery versus reaction pressure at different WHSV.

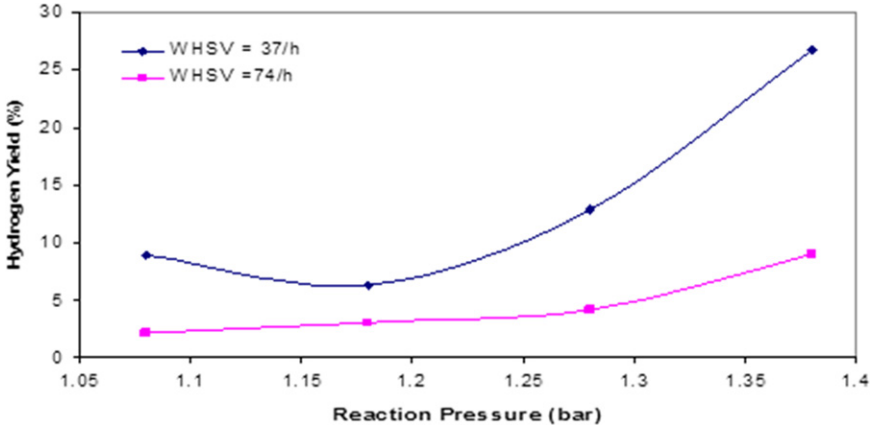

Fig. 9. Hydrogen yield versus reaction pressure at different WHSV.

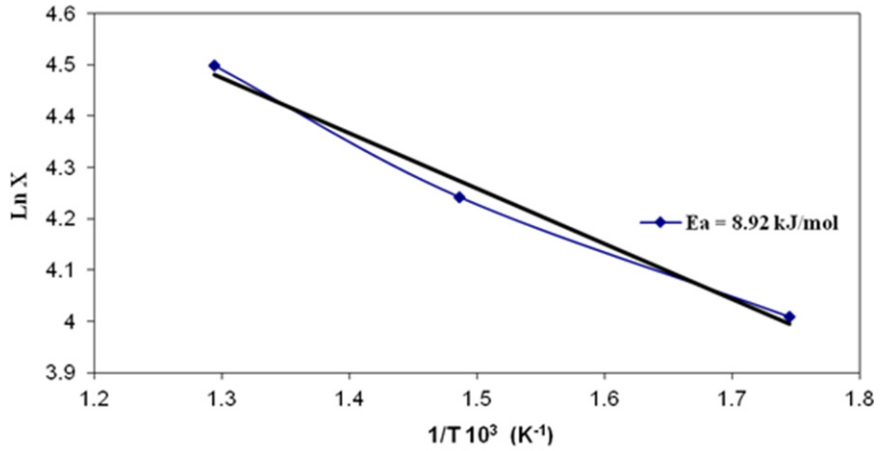

Fig. 10. Temperature dependence of ethanol conversion.

Table 4
Activation energy for permeation of hydrogen through a palladium-based membrane via an ethanol steam reforming process.

Pd-based membrane	Thickness (μm)	P (kPa)	T (K)	E_a (kJ mol^{-1})	Q_0 (mol m^{-1} s^{-1} Pa$^{-0.5}$)	Reference
Pd–Al_2O_3	7.146	108–138	573–773	8.92	1.31×10^{-9}	This work
Pd–Ag	50	100–500	673	8.58	3.61×10^{-8}	[22]
Pd–Ag	150	100–800	573–723	5,52	4.14×10^{-8}	[28]

where Q_0 is a pre-exponential factor (mol m^{-1} s^{-1} bar$^{-0.5}$), E_a is the activation energy (J mol^{-1}), R is the universal gas constant (8.314 J mol^{-1} K^{-1}), and T is the absolute temperature (K). The Arrhenius plot of the ethanol conversion is shown in Fig. 10. Increasing temperature had a good influence by increasing the ethanol conversion and gives an activation energy of 8.92 kJ mol^{-1} in a temperature range of 573–773 K. It does mean that the ethanol steam reforming reaction is dominant at higher temperature. Comparison of the activation energy for hydrogen permeation through the Pd-based membrane obtained from this work with previous work is shown in Table 4. The value of the activation energy for the hydrogen permeation was closely similar to that reported by Iulianelli et al. [22] but quite different from that reported by Tosti et al. [28]. The hydrogen permeabilities reported by Iulianelli et al. [22] and Tosti et al. [28] were very similar. The lower permeability for this membrane may be attributed to resistance of two ceramic layers, γ-alumina dan α-alumina.

4. Conclusions

Hydrogen was produced by an ethanol steam reforming process in a Pd–alumina MR at various reaction pressure and WHSV. A value of $n=0.5$ was obtained, implying that the mechanism of hydrogen transport through the Pd–alumina membrane follows Sieverts' law which suggests that the permeation rate of hydrogen was dependent only on bulk phase diffusion. A lower WHSV increased ethanol conversion and CO_2 selectivity, and decreased CO selectivity. Increasing pressure had a positive effect on the ethanol steam reforming reaction, where higher increments were seen for ethanol conversion, hydrogen recovery, hydrogen yield and hydrogen selectivity. The ethanol conversion, hydrogen recovery, hydrogen yield and hydrogen selectivity were 61.5%, 42.82%, 26.75&, and 92.6%, respectively, at a pressure of 1.38 bar, and WHSV of 37 h^{-1}. The activation energy and permeability for hydrogen permeation were 8.92 kJ mol^{-1} and 1.31×10^{-9} (mol m^{-1} s^{-1} Pa$^{-0.5}$), respectively.

Acknowledgements

The authors gratefully acknowledge the financial support from Universiti Kebangsaan Malaysia under grant UKM-GUP-TK-08–17-321.

References

[1] A. Li, J.R. Grace, C.J. Lim, Preparation of thin Pd-based composite membrane on planar metallic substrate Part I: pre-treatment of porous stainless steel substrate, Journal of Membrane Science 298 (2007) 175–181.
[2] J. Okazaki, T. Ikeda, D.A.P. Tanaka, K. Sato, T.M. Suzuki, F. Mizukami, An investigation of thermal stability of thin palladium–silver alloy membranes for high temperature hydrogen separation, Journal of Membrane Science 366 (2011) 212–219.
[3] C.Y. Yu, D.W. Lee, S.J. Park, L.K.Y. Lee, K.H. Lee, Study on a catalytic membrane reactor for hydrogen production from ethanol steam reforming, International Journal of Hydrogen Energy 34 (2009) 2947–2954.

[4] M. Ni, D.Y.C. Leung, M.K.H. Leung, A review on reforming bio-ethanol for hydrogen production, International Journal of Hydrogen Energy 32 (2007) 3238–3247.
[5] S. Tosti, Overview of Pd-based membranes for producing pure hydrogen and state of art at ENEA laboratories, International Journal of Hydrogen Energy 35 (2010) 12650–12659.
[6] W. Chen, X. Hu, R. Wang, Y. Huang, On the assembling of Pd/ceramic composite membranes for hydrogen, Separation, Separation and Purification Technology 72 (2010) 92–97.
[7] S.K. Ryi, N. Xu, A. Li, C.J. Lim, J.R. Grace, Electroless Pd membrane deposition on alumina modified porous Hastelloy substrate with EDTA-free bath, International Journal of Hydrogen Energy 35 (2010) 2328–2335.
[8] Y.H. Chi, P.S. Yen, M.S. Jeng, S.T. Ko, T.C. Lee, Preparation of thin Pd membrane on porous stainless steel tubes modified by a two-step method, International Journal of Hydrogen Energy 35 (2010) 6303–6310.
[9] R. Del Colle, C.A. Fortulan, S.R. Fontes, Manufacture and characterization of ultra and microfiltration ceramic membranes by isostatic pressing, Ceramics International 37 (2011) 1161–1168.
[10] J. Okazaki, T. Ikeda, D.A.P. Tanaka, T.M. Suzuki, F. Mizukami, In situ high-temperature X-ray diffraction study of thin palladium/α-alumina composite membranes and their hydrogen permeation properties, Journal of Membrane Science 335 (2009) 126–132.
[11] D.A.P. Tanaka, M.A.L. Tanco, S.I. Niwa, Y. Wakui, F. Mizukami, T. Namba, T.M. Suzuki, Preparation of palladium and silver alloy membrane on a porous α-alumina tube via simultaneous electroless plating, Journal of Membrane Science 247 (2005) 21–27.
[12] E. David, J. Kopac, Development of palladium/ceramic membranes for hydrogen separation, International Journal of Hydrogen Energy 36 (2011) 4498–4506.
[13] Y. Huang, R. Dittmeyer, Preparation of thin palladium membranes on a porous support with rough surface, Journal of Membrane Science 302 (2007) 160–170.
[14] N. Agoudjil, S. Kermadi, A. Larbot, Synthesis of inorganic membrane by sol–gel process, Desalination 223 (2008) 417–424.
[15] A.L. Ahmad, N.N.N. Mustafa, Sol–gel synthesized of nanocomposite palladium–alumina ceramic membrane for H_2 permeability: preparation and characterization, International Journal of Hydrogen Energy 33 (2007) 2010–2021.
[16] M.R. Othman, J. Kim, Permeation characteristics of H_2, N_2, and CO_2 in a binary mixture across meso-porous Al_2O_3 and Pd–Al_2O_3 asymmetric composite, Microporous and Mesoporous Materials 112 (2008) 403–410.
[17] A.L. Ahmad, M.R. Othman, H. Mukhtar, H_2 separation from binary gas mixture using coated alumina–titania membrane by sol–gel technique at high-temperature region, International Journal of Hydrogen Energy 29 (2004) 817–828.
[18] T.V. Gestel, C. Vandecasteele, A. Buekenhoudt, C. Dotremont, J. Luyten, R. Leysen, B.V. der Bruggen, G. Maes, Alumina and titania multilayer membranes for nanofiltration: preparation, characterization, and chemical stability, Journal of Membrane Science 207 (2002) 73–89.
[19] Y.H. Ma, B.C. Akis, M.E. Ayturk, F. Guazzone, E.E. Engwall, I.P. Mardilovich, Characterization of intermetallic diffusion barrier and alloy formation for Pd/Cu and Pd/Ag porous stainless steel composite membrane, Industrial and Engineering Chemistry Research 43 (2004) 2936–2945.
[20] H. Lim, Y. Gu, S.T. Oyama, Reaction of primary and secondary products in a membrane reactor: studies of ethanol steam reforming with a silica–alumina composite membrane, Journal of Membrane Science 351 (2010) 149–159.
[21] A. Basile, P. Pinacci, A. Iulianelli, M. Broglia, F. Drago, S. Liguori, T. Longo, V. Calabro, Ethanol steam reforming reaction in a porous stainless steel supported palladium membrane reactor, International Journal of Hydrogen Energy 36 (2010) 2029–2037.
[22] A. Iulianelli, A. Basile, An experimental study on bio-ethanol steam reforming in a catalytic membrane reactor. Part I: temperature and sweep-gas flow configuration effects, International Journal of Hydrogen Energy 35 (2010) 3170–3177.
[23] M.R. Othman, I.S. Sahadan, On the characteristics and hydrogen adsorption properties of a Palladium/γ-Al_2O_3 prepared by sol–gel method, Microporous and Mesoporous Materials 91 (2006) 145–150.
[24] A. Basile, A. Iulianelli, T. Longo, S. Liguori, M. De Falco, Pd-based Selective Membrane, State-of-the-Art, in: En: M. De Falco, L. Marrelli, G. Iaquaniello (Eds.), Membrane Reactors for Hydrogen Production Processes, Springer, Londres, 2011.
[25] J.P. Collins, J.D. Way, Preparation and characterization of a composite palladium ceramic membrane, Industrial and Engineering Chemistry Research 32 (1993) 3006.
[26] F. Guazzone, Y.H. Ma, Leak growth mechanism in composite Pd membranes prepared by the electroless deposition method, AIChE Journal 54 (2) (2007) 487–494.
[27] R. Dittmeyer, V. Hollein, K. Daub, Membrane reactors for hydrogenation and dehydrogenation processes based on supported palladium, Journal of Molecular Catalysis A: Chemical 173 (2001) 135–184.
[28] S. Tosti, M. Fabbricino, A. Moriani, G. Agatiello, C. Scudieri, F. Borgognoni, A. Santucci, Pressure effect in ethanol steam reforming via dense Pd-based membranes, Journal of Membrane Science 37 (2011) 65–74.